JCTC Journal of Chemical Theory and Computation

Article

pubs.acs.org/JCTC

Energy Diagrams for Water Oxidation in Photosystem II Using Different Density Functionals

Per E. M. Siegbahn* and Margareta R. A. Blomberg

Department of Organic Chemistry, Arrhenius Laboratory, Stockholm University, SE-106 91 Stockholm, Sweden

Supporting Information

ABSTRACT: The full sequence of intermediates in the water oxidation process in photosystem II has recently been characterized by model calculations, in good agreement with experiments. In the present paper, the energy diagram obtained is used as a benchmark test for several density functionals. Only the results using B3LYP with 15% or 20% show good agreement with experiments. The other functionals tried show errors for some energy levels as large as 20−30 kcal/mol. The reason for these large errors is that the error for three consecutive oxidations of Mn(III) to Mn(IV) accumulates as the cluster is oxidized.

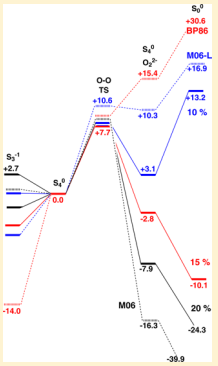

I. INTRODUCTION

The mechanism for water oxidation in nature has during the past five years been characterized almost completely by model calculations.[1,2] The DFT structure for the oxygen-evolving catalyst (OEC) suggested in 2008[3] is essentially identical to a recent high-resolution structure.[4] The detailed structure for the intermediate S_2 state was confirmed two years ago by a joint EPR and DFT study.[5] The oxyl−oxo coupling mechanism for O−O bond formation in the S_4 state suggested by DFT in 2006[6] has recently been confirmed by substrate water exchange experiments.[7] Also, the detailed energetics from S_0 back to S_0 has been obtained by DFT model studies and the use of limited empirical information.[2] The resulting energy diagram agrees in all parts with what is available experimentally. That information is, for example, the characterization of intermediate states at different oxidation levels. In all transitions between observed states, except one, both an electron and a proton leave the OEC. In the S_1 to S_2 transition, only an electron leaves. Already these general observations, available for decades, give quite strong restrictions on the potential surface.

Because energy diagram for water oxidation in PSII is so well established, it represents an excellent benchmark test for different density functionals. In particular, the water oxidation process involves a number of redox steps, which are known to be difficult to describe by DFT or any other method. In the present paper, entire diagrams will be presented for a number of commonly used functionals. The results are compared to previous results and to the experiments.

II. METHODS AND MODELS

In the present tests of density functionals, the same geometries as reported previously[2] were used. All the directly binding amino acids were included, four second shell ones and the chloride and five water molecules forming a surrounding hydrogen bonding network, altogether about 200 atoms. Also, the zero point energies were taken to be the same as before. The energies for the different functionals were computed using the large (cc-pvtz(-f), lacv3p+ for the metals) basis set. The solvation effects were computed for each functional using a smaller (lacvp*) basis set and with a dielectric constant of 6.0 as before. The sensitivity of the present results (only relative values) to the choice of dielectric constant is very small.[3] Dispersion effects using the D2-correction[8] were added except for the M06 and M06-L functionals because they already include these effects. For one state (S_4) in the diagrams, an energy lowering spin-coupling correction of 2.8 kcal/mol has been added. Entropy effects are explicitly added only in the step where O_2 is released, where it is assumed that a translational entropy of 10.7 kcal/mol is gained. When water enters from the bulk, an empirical cost of 14 kcal/mol is used. All calculations were done using Jaguar.[9]

In the previous study, the B3LYP hybrid functional was used[10] but with only 15% exact exchange, also called B3LYP*.[11] In the present study, the M06 hybrid functional,[12] M06-L nonhybrid functional,[13] and BP86 nonhybrid functional[14,15] were used. In addition, B3LYP was used with the normal value of 20% for the exact exchange and also with only 10%.

As in the previous study, the relative energies for all functionals of removing the (H^+,e^-)-couples were fitted to the experimental reaction energy for the entire process of 51.5 kcal/mol at pH 7. There is only one way to do this, and after this fitting, every second level in the energy diagrams is fixed. To obtain also the energies for the other levels, a single

Received: November 5, 2013
Published: December 4, 2013

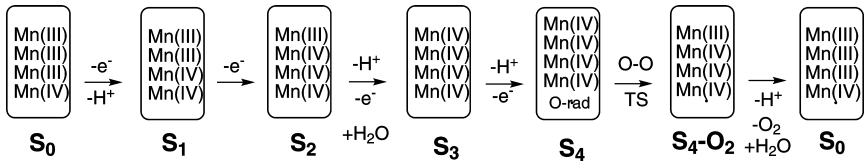

Figure 1. S state sequence for water oxidation in PSII.

parameter has to be chosen for each diagram. This value is different for all functionals and is fitted to make the best possible agreement with the experimental results. After this fitting, the pK_a values (relative to pH 7) and redox potentials (relative to the redox potential of the oxidant P_{680} of 1.25 V[16,17]) are determined. In addition, also from the previous study, at two points in the diagram an electrostatic effect from the ionized oxidant P^+_{680} of −5 kcal/mol was included. These two points are for the proton release in the S_2 to S_3 and the S_3 to S_4 steps. The details of the parametrization, with examples, are given for the different functionals in the Supporting Information.

III. RESULTS

Before the comparison between the functionals is made, the previous results will be briefly discussed in relation to what is known experimentally. The sequence of events is shown in Figure 1. The intermediates are termed S states, and the first one is S_0, which has three Mn(III) and one Mn(IV), each one high-spin coupled. In the calculations, the spins on the Mn atoms are ferromagnetically coupled, except in S_4 where two manganese centers have to be antiferromagnetically coupled.[2] In each S transition, an electron is sent to the oxidant P^+_{680}, and for all transitions except one, S_1 to S_2,[18,19] a proton is sent to bulk water at the lumenal side. In the first three steps, Mn(III) is oxidized to Mn(IV). In the fourth step, model calculations suggest that an oxyl radical is formed rather than a further oxidation of Mn(IV) to Mn(V). For each S state, one intermediate has been observed with an exergonicity in the transition between the states larger than 3−5 kcal/mol. In both the S_2 to S_3 and S_3 to S_4 transitions, a proton is observed to leave the cluster before the cluster is oxidized.[20] This is interpreted as a repulsion between the proton on the cluster and the nearby oxidized Tyr^+_Z, which is formed by an electron transfer from Tyr_Z to P^+_{680}. This means that before P_{680} is oxidized, the proton should be stable on the cluster by at least 2−3 kcal/mol, but afterward it should be unstable by 2−3 kcal/mol. An ad hoc repulsion of 5 kcal/mol is introduced for all functionals. For the O−O bond formation step, it is known that it takes on the order of a millisecond (corresponding to a barrier of about 13 kcal/mol). The immediate S_4 reactant has not been observed. The exergonicity in the final S transition from S_3 to S_0 should be larger than 5 kcal/mol.

The comparison between the previous results (B3LYP-15%) and the M06 hybrid and M06-L nonhybrid functionals is shown in Figure 2. The energy levels are marked as S^m_n, where n is the oxidation level and m the charge of the state. For each S_n-state, there are thus two levels. The results using the BP86 nonhybrid functional does not fit into the figure but will be discussed in parallel.

The previous calculations[2] are in quite good agreement with the above experimental observations. The stoichiometries (H^+,e^- releases) of the S transitions are correct, and the exergonicities are reasonable. The initial energetics of the two last S transitions are in agreement with the strong restrictions

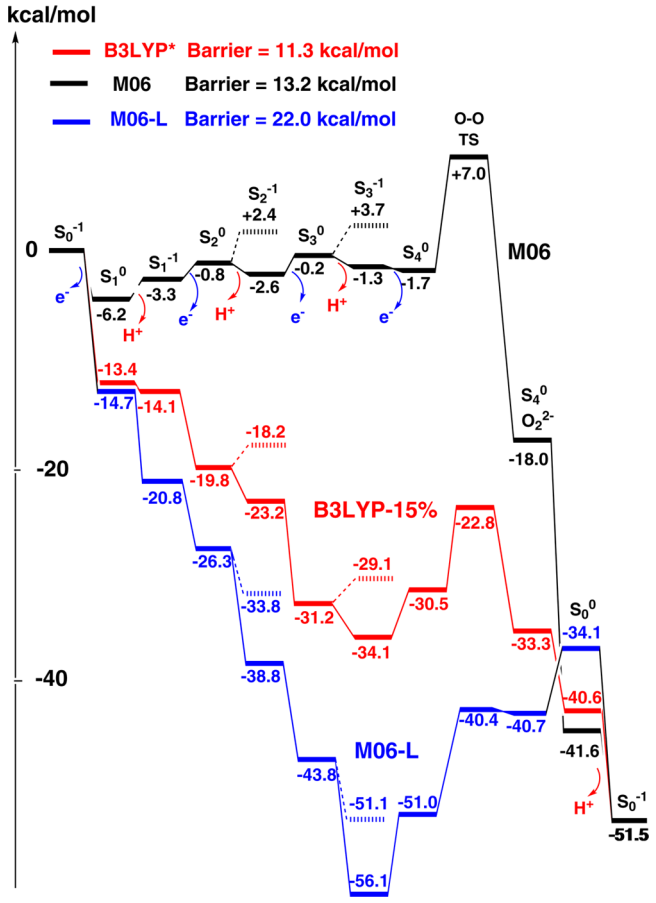

Figure 2. Comparison of the water oxidation energy profiles for different DFT functionals. The results are computed using the same assumptions in the three cases (see text).

indicated by the experiments. The rate of O−O bond formation is within milliseconds as required. In another study,[21] the kinetics of the proton transfer steps on the cluster was also found to be within the required milliseconds.

As clearly shown in Figure 2, both the M06 and M06-L diagrams differ substantially from the B3LYP-15% one, and thereby also from the experiments. M06-L has too large exergonicities in the oxidations from Mn(III) to Mn(IV) and M06 too small. Because the proton affinities are quite similar between the functionals, all the error comes from the ionization energies. For the oxidation from Mn(III) to Mn(IV), it is about 10 kcal/mol too large for M06 and about 10 kcal/mol too small for M06-L. Because this ionization occurs three times, the error goes all the way to around +30 kcal/mol for M06 and to about −20 kcal/mol for M06-L in S_3. Somewhat surprisingly, the fitting of the results to the total experimental exergonicity of −51.5 kcal/mol does not help much. The reason is the step where the O−O bond is formed, in which an Mn(IV) is reduced to Mn(III) and where the error goes the opposite way. The calculated reaction energy for this step cannot be corrected

dx.doi.org/10.1021/ct401039h | J. Chem. Theory Comput. 2014, 10, 268−272

by the fitting and limits the possibilities to correct the other steps without destroying too much of the rest of the diagram. The rate-limiting barrier for M06, on the other hand, is quite reasonable, 13.2 compared to the B3LYP-15% value of 11.3 kcal/mol, while the barrier for M06-L is too high by about 10 kcal/mol. There are two reasons for this. First, the resting S_3-state has moved all the way down to −56.1 kcal/mol for M06-L by the too easy oxidations in the first three steps. Second, the energy continues to go up for M06-L also after O−O bond formation to the highest point at −34.1 kcal/mol for S_0^0. The energy of the S_3-state is actually lower than the final state, which is also in disagreement with the experiments. It is possible to change the barrier from S_3^{-1} to S_0^0 with a different parametrization. However, this will automatically lead to an even lower energy of S_3^{-1} with respect to the final point and will thus not lead to an overall improvement of the potential curve. In contrast to M06-L, the M06 diagram is too flat, leading to a resting S_1-state for O−O bond formation.

The BP86 results were not included in the diagram because they would fall outside the margins used. BP86 gives rather similar results to M06-L but with somewhat larger errors. This means that the energy goes down all the way to −76.1 kcal/mol for S_3 using essentially the same fitting parameter as for M06-L. The rate-limiting barrier becomes as high as 45 kcal/mol because as M06-L the energy continues to go up all the way to the S_0^0 state, at −31.5 kcal/mol in this case. The computed results for BP86 are given in the Supporting Information.

It seems clear from the results discussed above that the amount of exact exchange matters strongly for the diagrams. To analyze the situation more systematically, results were computed for B3LYP with three different values for the exact exchange, 10%, 15%, and 20%, with results shown in Figure 3. As a general rule of thumb, the ionization potential going from Mn(III) to Mn(IV) increases by 1 kcal/mol for each percent increase of the exact exchange. Something similar has been pointed out before for copper-containing complexes.[22] The diagrams show that 10% is not enough for agreement with the experiments, giving a lowest point of −53.8 kcal/mol, which is below the final state. It is somewhat more difficult to choose the best of the functionals with 15% and 20%. There are mainly two reasons to select the functional with 15% to be the best one. First, the results with 20% would indicate that only an electron is released in the S_0 to S_1 transition, in contrast to experimental observations where also a proton is released. Second, the peroxide structure is substantially lower in energy than the S_3 state using 20%, indicating that the peroxide ought to have been detected experimentally, which has not been the case. The peroxide is surrounded by rather high barriers, so the lifetime should be enough for observation. Also, the initial proton release patterns in the S_2 to S_3 and S_3 to S_4 transitions are not quite in agreement with the experiments. These rather limited differences were the reason for choosing the functional with 15% in the previous studies. It is important to note that the present systems throughout the diagram have high-spin coupling of the Mn d-electrons, which limits near-degeneracy (multi-reference) effects. High-spin coupling of the d-electrons is very common in biology and is the rule for manganese and nonheme iron complexes in general. For systems with more pronounced near-degeneracy effects, like heme-complexes, it is not unlikely that a value lower than 15% could be more optimal.[23] As a general rule, it is suggested here that a variation of the exchange is a more systematic procedure to learn more about the optimal functional than what has generally been done

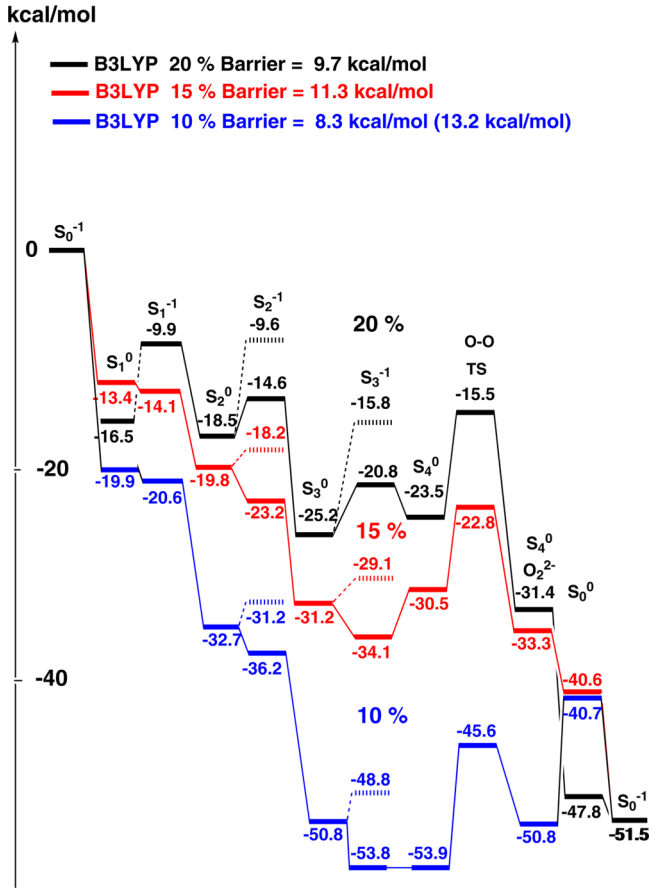

Figure 3. Comparison of the water oxidation energy profiles for B3LYP-type functionals with different amounts of exact exchange. For the case of 10%, two barriers are given: one for just going to the O−O bond formation TS and the other one going to the S_0^0 state. The results are computed using the same assumptions in the three cases (see text).

before when a large number of fundamentally different functionals have been compared to select the best one.

In the final comparison between different functionals made here, only the part between S_3^{-1} and S_0^0 is selected (Figure 4). The purpose is to show more clearly the sensitivity of this critical part of the mechanism to the choice of functional. In this case, the energy for S_4^0 is set to zero. One quite striking feature of this figure is that the O−O bond formation barrier is very similar between the functionals. The lowest barrier of 7.7 kcal/mol is found for B3LYP-15% and the highest one of 10.6 kcal/mol for M06-L. With such a small difference, it is likely that any functional would have predicted the oxo−oxyl mechanism as the preferred one. This is gratifying because the mechanism for O−O bond formation is the most important aspect of the entire diagram. However, both after and before this step, there are very big differences between the functionals, as already mentioned above. In particular, the nonhybrid functionals give very discouraging results. Before the O−O bond formation, the oxidative side, the energies are much too low, and afterward on the reductive side they are much too high due to the error in the Mn(III) to Mn(IV) redox potential.

It should finally be added that in many earlier comparisons between functionals very different conclusions concerning the adequacy of B3LYP have been drawn for transition metal complexes. A few remarks can be given concerning these earlier comparisons. First, most of them were made some time ago

dx.doi.org/10.1021/ct401039h | J. Chem. Theory Comput. 2014, 10, 268−272

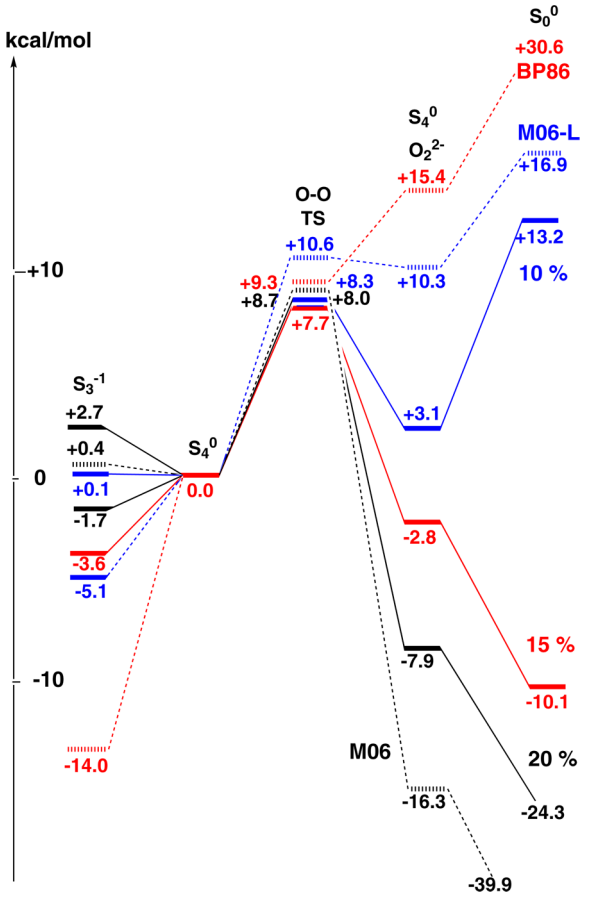

Figure 4. Comparison of the water oxidation energy profiles from S_3 to S_0 using different functionals. For these diagrams, the energy for the S_4 state was set to zero for all functionals. The results are computed using the same assumptions in all cases (see text).

before the inclusion of dispersion effects became mandatory, as they are now. For example, a huge error of B3LYP was demonstrated for a Grubbs II metathesis complex containing ruthenium.[24] However, in a later study, it was shown that this error was essentially removed when dispersion was added.[25] In one case, the ligand dissociation energy went from −1 kcal/mol to +25 kcal/mol in good agreement with the experiments. In another study,[26] it was shown that previously demonstrated large errors disappeared for methyl−cobalamine[27,28] and for copper dimer complexes[29] when dispersion was added. It was also shown that dispersion effects are only large for metal−ligand binding steps. In all the other steps, like covalent bond-cleavage or bond-formation, they were essentially zero. Finally, failures of B3LYP for small unsaturated metal complexes are well documented.[30] However, these systems are completely different in nature from the saturated complexes discussed here. For the small systems, near degeneracy and multi-reference effects are very common. They are much more difficult to correct for, but this can be done in some cases. The very poor binding curve for Cr_2 is moved into nearly perfect agreement with the experiments by using a spin-coupling correction.[31] This type of correction is rarely needed in saturated systems. However in the present systems, there is a small correction of this type at one place of 2.8 kcal/mol (see Section II). Dispersion effects are on the other hand very small for Cr_2.

IV. CONCLUSIONS

In previous studies of water oxidation in photosystem II, an energy diagram for the entire process has been calculated using the B3LYP-15% functional. The results have been demonstrated to be in agreement with experiments in all parts where comparisons are possible. In the present study, this diagram is compared to the ones obtained for other functionals. Apart from the fact that the local O−O bond formation barrier is quite similar between the functionals, there are sometimes very big differences for other parts of the diagram. In particular, the ionization potential (redox potential) going from Mn(III) to Mn(IV) (high-spin) is very sensitive. This energy is too small by about 10 kcal/mol for the nonhybrid functionals M06-L and BP86 and too large for the hybrid functional M06 by about the same amount. Because this oxidation occurs three times in the diagram, the effects are very large for the final shape of the diagram. On the other hand, proton affinities are much more stable differing by only a few kcal/mol.

To analyze the difference between hybrid and nonhybrid functionals, the amount of exact exchange was varied between 10% and 20% for the B3LYP functional. It turns out that the redox potential for Mn(III) increases by about 1 kcal/mol for each percent of exact exchange that is added. The best results are found for B3LYP-15% with the ones for 20% only slightly worse. The results for 10% are not satisfactory. It is suggested that varying the amount of exact exchange in B3LYP is generally a more systematically informative procedure than comparing fundamentally different functionals.

■ ASSOCIATED CONTENT

Ⓢ Supporting Information

Calculated ionization potentials and proton affinities for each functional and details of the present parametrization as well as how the diagrams are set up from the computed values. This material is available free of charge via the Internet at http://pubs.acs.org.

■ AUTHOR INFORMATION

Corresponding Author

*E-mail: ps@physto.se.

Notes

The authors declare no competing financial interest.

■ REFERENCES

(1) Siegbahn, P. E. M. *Acc. Chem. Res.* **2009**, *42*, 1871−1880.
(2) Siegbahn, P. E. M. *Biochim. Biophys. Acta* **2013**, *1827*, 1003−1019.
(3) Siegbahn, P. E. M. *Chem.—Eur. J.* **2008**, *27*, 8290−8302.
(4) Umena, Y.; Kawakami, K.; Shen, J.-R.; Kamiya, N. *Nature* **2011**, *473*, 55−60.
(5) Ames, W.; Pantazis, D. A.; Krewald, V.; Cox, N.; Messinger, J.; Lubitz, W.; Neese, F. *J. Am. Chem. Soc.* **2011**, *133*, 19743−19757.
(6) Siegbahn, P. E. M. *Chem.—Eur. J.* **2006**, *12*, 9217−9227.
(7) Rapatskiy, L.; Cox, N.; Savitsky, A.; Ames, W. M.; Sander, J.; Nowacyzk, M. M.; Rögner, M.; Boussac, A.; Neese, F.; Messinger, J.; Lubitz, W. *J. Am. Chem. Soc.* **2012**, *134*, 16619−16634.
(8) Schwabe, T.; Grimme, S. *Phys. Chem. Chem. Phys.* **2007**, *9*, 3397−3406.
(9) *Jaguar 7.9*, Schrödinger, L.L.C., Portland, OR, 1991−2013).
(10) Becke, A. D. *J. Chem. Phys.* **1993**, *98*, 5648−5652.
(11) Reiher, M.; Salomon, O.; Hess, B. A. *Theor. Chem. Acc.* **2001**, *107*, 48−55.
(12) Zhao, Y.; Truhlar, D. G. *Theor. Chem. Acc.* **2008**, *120*, 215−241.
(13) Zhao, Y.; Truhlar, D. G. *Acc. Chem. Res.* **2008**, *41*, 157−167.

(14) Becke, A. D. *Phys. Rev. A* **1988**, *38*, 3098−3100.
(15) Perdew, J. P. *Phys. Rev. B* **1986**, *33*, 8822−8824.
(16) Diner, B. A. *Biochim. Biophys. Acta* **2001**, *1503*, 147−163.
(17) Rappaport, F.; Lavergne, J. *Biochim. Biophys. Acta* **2001**, *1503*, 246−259.
(18) Förster, V.; Junge, W. *Photochem. Photobiol.* **1985**, *41*, 183−190.
(19) Renger, G. *Physiologica Plantarum* **1997**, *100*, 828−841.
(20) (a) Haumann, M.; Liebisch, P.; Müller, C.; Barra, M.; Grabolle, M.; Dau, H. *Science* **2005**, *310*, 1019−1021. (b) Klauss, A.; Haumann, M.; Dau, H. *Proc. Natl. Acad. Sci* **2012**, *109*, 16035−16040.
(21) Siegbahn, P. E. M. *J. Am. Chem. Soc.* **2013**, *135*, 9442−9449.
(22) Cramer, C. J.; Wloch, M.; Piecuch, P.; Puzzarini, C.; Gagliardi, L. *J. Phys. Chem. A* **2006**, *110*, 1991−2004.
(23) Jensen, K. P.; Cirera, J. *J. Phys. Chem. A* **2009**, *113*, 10033−10039.
(24) Zhao, Y.; Truhlar, D. G. *Org. Lett.* **2007**, *9*, 1967−1970.
(25) Minemkov, Y.; Occhipinti, G.; Jensen, V. R. *J. Phys. Chem. A* **2009**, *113*, 11833−11844.
(26) Siegbahn, P. E. M.; Blomberg, M. R. A.; Chen, S.-L. *J. Chem. Theory Comput.* **2010**, *6*, 2040−2044.
(27) Jensen, K. P.; Ryde, U. *J. Phys. Chem. A* **2003**, *107*, 7539−7545.
(28) Kozlowski, P. M.; Kamachi, T.; Toraya, T.; Yoshizawa, K. *Angew. Chem., Int. Ed.* **2007**, *46*, 980−983.
(29) (a) Lewin, J. L.; Heppner, D. E.; Cramer, C. J. *J. Biol. Inorg. Chem.* **2007**, *12*, 1221−1234. (b) Gherman, B. F.; Cramer, C. J. *Coord. Chem. Rev.* **2009**, *253*, 723−753.
(30) Zhang, W.; Truhlar, D. G.; Tang, M. *J. Chem. Theory Comput.* **2013**, *9*, 3965−3977.
(31) Siegbahn, P. E. M.; Blomberg, M. R. A. *Intern. J. Quantum Chem.* **2010**, *110*, 317−322.